High power lithium ion polymer batteries (IV): Nano-sized cathode materials manufactured in a single synthetic step using united eutectic self-mixing method

안 욱 · 라 동 일 · 이 범 재 · 한 규 승

Abstract

Nano-sized cathode materials for high power lithium ion polymer battery are easily and economically prepared using united eutectic self-mixing method without any artificial mixing procedures of reactants and ultra-miniaturization of products. While the micro-sized $LiNi_{0.7}Co_{0.3}O_2$ exhibits the discharge capacities of 167.8 mAh/g at 0.1C and 142.5 mAh/g at 3.0C, those of the nano-sized $LiNi_{0.7}Co_{0.3}O_2$ are 170.8 mAh/g at 0.1C and 159.3 mAh/g at 3.0C. In the case of $LiCoO_2$, the micro-sized $LiCoO_2$ exhibits the discharge capacities of 134.8 mAh/g at 0.1C and 118.6 mAh/g at 5.0C. Differently, the nano-sized $LiCoO_2$ exhibits the discharge capacities of 137.2 mAh/g at 0.1C and 131.7 mAh/g at 5.0C.

1. Introduction

From the dawning of Li ion batteries, lithiated

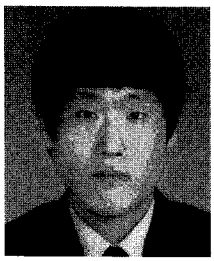

안 욱

1997~ 2005 충남대학교 정밀공업화학과
2005~ 현재 충남대학교 공업화학과 석사

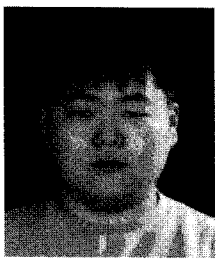

라동일

1997~ 2004 충남대학교 정밀공업화학과
2004~ 충남대학교 공업화학과 석사

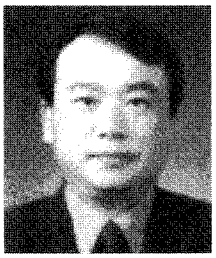

이범재

1973~ 1977 서울대학교 공과대학 공업화학과
1980~ 1982 충남대학교 화학과 석사
1986~ 1991 The University of Akron, Polymer Science, Ph.D
1977~ 1995 국방과학연구소(선임연구원)
1998~ 2001 대전광역시 교육청 (기획평가자문위원)
2002~ 2004 한국공업화학회 대전지부 총무이사
2002~ 현재 충남대학교 공과대학 정밀공업화학과(정교수)
2004~ 2005 Cornell University (Visiting Scholar)

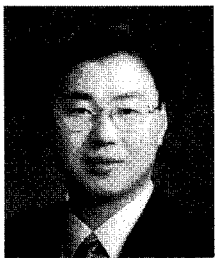

한규승

1989 서울대학교 화학과 학사
1991~ 1992 프랑스 보르도 제1대학 물리학 석사
1992~ 1996 프랑스 보르도 제1대학 재료과학과 박사
1996~ 1999 일본 동경공대 재료공학과 시간 강사
1999 미국 로렌스버클리 국립연구소 연구원
1999~ 현재 충남대학교 정밀공업화학과 부교수

transition metal oxide is ceaselessly used as the cathode material for almost all commercialized lithium rechargeable batteries due to its suitable performances such as high energy density, ease of manufacture, etc. In the past two decades, a wealth of research on lithiated transition metal oxide has achieved advances in technology in terms of synthetic techniques, electrochemical properties, effect of doping and/or coating, thermal stability, etc. Nonetheless, to accommodate the increasing user's demands especially in the fields of multi-functioned mobile electronics and high power applications such as electric vehicle, intensive efforts seem to be concentrated to good battery performance at high rates. The diffusion of lithium ion in the cathode material, as a function of concentration gradient, must be fast enough to grant a good rate capacity. Thus, to obtain high power lithium ion polymer batteries, cathode material needs to be encouraged by ultra-miniaturization in a nano-size. Nano-sized cathode materials can be obtained by controlling of crystal nucleation and crystal growth.

The preparation of cathode materials using eutectic self-mixing method and the good battery performances of the prepared cathode materials are described in our previous report.[1-7] Using this method, the manufacturing procedure is easily made up just thermal reaction at high temperature in air without any pulverization, grinding, particle morphology controlling, and particle size controlling of reactants as well as products. When lithium and transition metal acetates are exposed to their eutectic temperature, they can be fluidized substances by themselves without any solvents and then spontaneously and homogenously mixed together.[1-7] In addition, it is found that the intermediate heat treatments of lithium and transition metal acetates are required to obtain the steady phase transition and the enhanced battery performances.[1-7]

Here, we present the results of the simple but successful preparation of nano-sized cathode materials in a single synthetic step using advanced eutectic self-mixing method, as well as a good example of how to accomplish material preparation and simultaneous ultra-miniaturization in a nano-size by design of the experimental conditions based on the elucidation of the reaction mechanism study.

2. Experimental

2.1 $LiNi_{0.7}Co_{0.3}O_2$

The preparation of nano-sized $LiNi_{0.7}Co_{0.3}O_2$ phase using united acetate self-mixing method was performed as follows: 0.105 mol of $LiCH_3CO_2 \cdot 2H_2O$, 0.07 mol of $Ni(CH_3CO_2)_2 \cdot 4H_2O$, and 0.03 mol of $Co(CH_3CO_2)_2 \cdot 4H_2O$ were heated consecutively at 130 ℃ for 50 min in air, 300 ℃ for 8 hrs in a fixed CO_2 pressure between 0.001 and 1.0 kgf/cm^2, and at 800 ℃ for 24 hrs in air with no artificial mixing nor intermittent cooling. When the acetates are exposed to 130 ℃, they are typically fluid substances and spontaneously and homogeneously mixed together. Separately, micro-sized $LiNi_{0.7}Co_{0.3}O_2$ was also prepared as follows: 0.105 mol of $LiCH_3CO_2 \cdot 2H_2O$, 0.07 mol of $Ni(CH_3CO_2)_2 \cdot 4H_2O$, and 0.03 mol of $Co(CH_3CO_2)_2 \cdot 4H_2O$ were heated consecutively at 130 ℃ for 50 min, 300 ℃ for 8 hrs, and at 800 ℃ for 24 hrs in air without an external CO_2 stream. Excess $LiCH_3CO_2 \cdot 2H_2O$ was used to compensate for the loss of Li during the heating.

2.2 $LiMn_2O_4$

Both 0.105 mol of $LiCH_3CO_2 \cdot 2H_2O$ and 0.2 mol of $Mn(CH_3CO_2)_2 \cdot 4H_2O$ were consecutively heated up to their eutectic temperature (70℃) for 40 min in air, 250 ℃ for 8 hr in a fixed CO_2 pressure between 0.001 and 1.0 kgf/cm^2, and 750 ℃ for 20 hr at a rate of 10 ℃/min in air without any intermittent cooling. Excess $LiCH_3CO_2 \cdot 2H_2O$ was used

to compensate for the loss of Li during the heating.

2.3 $LiCoO_2$

To prepare nano-sized $LiCoO_2$, both 0.105 mol of $LiCH_3CO_2 \cdot 2H_2O$ and 0.1 mol of $Co(CH_3CO_2)_2 \cdot 4H_2O$ were heated consecutively at 80 ℃ for 40 min in air, 270 ℃ for 8 hr in a fixed CO_2 pressure between 0.001 and 1.0 kgf/cm^2, and 900 ℃ for 20 hr in air without any artificial mixing procedures and intermittent cooling. Separately, micro-sized $LiCoO_2$ was also prepared as follows: 0.105 mol of $LiCH_3CO_2 \cdot 2H_2O$ and 0.1 mol of $Co(CH_3CO_2)_2 \cdot 4H_2O$ were heated consecutively at 80 ℃ for 40 min, 350 ℃ for 8 hr, and 900 ℃ for 20 hr in air without an external CO_2 stream. Excess $LiCH_3CO_2 \cdot 2H_2O$ was used to compensate for the loss of Li during the heating.

2.4 Characterization

Thermal analysis of the acetates was performed at a rate of +1 ℃/min, from room temperature to 1000 ℃, in air using SDT 2960 TG-DTA (TA Instruments). X-ray diffraction (XRD) pattern analyses were achieved by using a Mac Science M03XHF^{22} diffractometer and Cu Kα radiation (λ = 1.5405 Å) operated with 30 mA and 40 kV. The diffractograms were recorded in the 2θ range of 5-90° with 0.02° intervals at a scanning rate of 2°/min. The scanning electron microscope (SEM) images of the prepared nano-sized $LiCoO_2$ and micro-sized $LiCoO_2$ were obtained using an Hitachi SEM S-4500. Electrochemical tests were carried out at room temperature using coin cells. The prepared cathode materials were mixed with 7 wt.% super-P carbon black and 8 wt.% poly-vinylidene fluoride (PVDF) binder dissolved in N-methyl-2-pyrrolidone (NMP) until a slurry was obtained. The slurry was laminated on an Al foil using a hot-roller press. The polymer electrolyte was a PVdF-HFP impregnated with 1.0 M $LiPF_6$ in EC/EMC (1:2). Lithium foil was used as anode; cell assembly was performed in an Ar-filled glove box; and cells were charged and discharged at 0.1C, 0.2C, 0.5C, 1.0C, 2.0C, 3.0C, and 5.0C.

3. Results and Discussion

In Figure 1, the TG-DTA curves of a mixture of $LiCH_3CO_2(2H_2O$, 0.7 $Ni(CH_3CO_2)2(4H_2O$, and 0.3 $Co(CH_3CO_2)2(4H_2O$ ascertain that the first weight-loss (experimental value of 30.8%) between room temperature and 100 ℃ together with small endothermic DTA peaks up to 80 ℃ correspond to the removal of hydrated $6H_2O$ (theoretical value of 30.8%). Beyond 100 ℃ up to 300 ℃, decomposition of the acetates results in the second weight loss of 39.8% and a large exothermic DTA peak at 282 ℃. This result is in accordance with the theoretical value, 40.2% for the release of $4.5H_2O$ and $6CO_2$, as well as the gain of $6.25O_2$. The exothermic heat generated from the decomposition of the acetates at 282 ℃ is predicted to be utilized as the lattice energy required for the formation of $LiNi_{0.7}Co_{0.3}O_2$ phase.

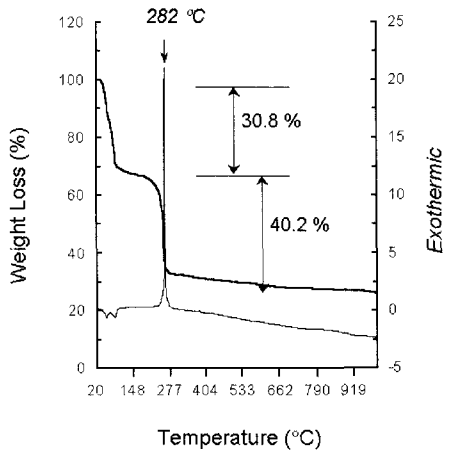

Figure 1. TG-DTA curves of a mixture of $LiCH_3CO_22H_2O$, 0.7 $Ni(CH_3CO_2)_2 \cdot 4H_2O$, and 0.3 $Co(CH_3CO_2)_2 \cdot 4H_2O$ measured at a heating rate of 1 ℃ min^{-1} under oxygen flow. The TG curve is shown as a thick line and DTA as a normal line.

Usually, the lattice energy is supplied by external heating. The reaction pathway can thus be given as follows:

$$LiCH_3CO_2 \cdot 2H_2O + 0.7\ Ni(CH_3CO_2)_2(4H_2O + 0.3\ Co(CH_3CO_2)_2(4H_2O \rightarrow LiNi_{0.7}Co_{0.3}(CH_3CO_2)_3 + 6H_2O \quad \text{(Eq. 1)}$$

$$LiNi_{0.7}Co_{0.3}(CH_3CO_2)_3 + 6.25O_2 \rightarrow LiNi_{0.7}Co_{0.3}O_2 + 4.5H_2O + 6CO_2 \quad \text{(Eq. 2)}$$

The temperature of 300 ℃ is the end-point for thermal weight loss, which means it is possible to prepare $LiNi_{0.7}Co_{0.3}O_2$ phase at a low temperature than 300 ℃. While the temperature of 300 ℃ is the end-point for all of thermal weight loss, endothermic and exothermic, the practical temperature of the second weight loss and the huge exothermic heat is 282 ℃. During the heating around 282 ℃, the decomposition of the acetates occurs, and 6 moles of CO_2 gas are simultaneously emitted. The crystallization process actually occurs in two stages, crystal nucleation and crystal growth. While the driving force for crystal growth is exclusively attached to just reaction temperature, the rate of crystal nucleation is the result of two competing factors; contributions of thermal motion and phase instability. Here, providing externally CO_2 gas during the self-emission of CO_2 gas promotes crystal nucleation and dispersion of crystal nuclei, but, at the same time, inhibits crystal growth.

TG-DTA curves of a mixture of $LiCH_3CO_2(2H_2O$ and $Mn(CH_3CO_2)_2(4H_2O$ in Figure 2 ascertain that the first weight-loss (experimental value of 29.8%) between room temperature and 170 ℃ together with small endothermic DTA peaks around 100 ℃ correspond to the removal of hydrated $10H_2O$ (theoretical value of 30.4%). Beyond 170 ℃ up to 250 ℃, decomposition of lithium acetate and manganese

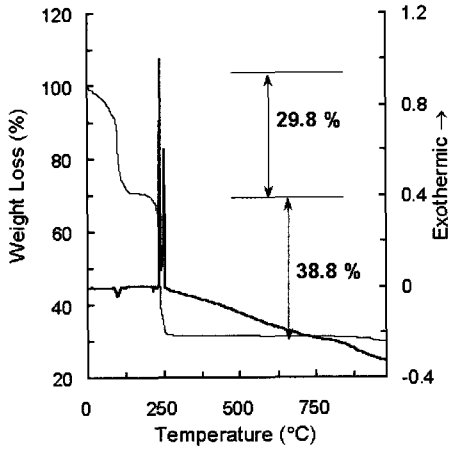

Figure 2. TG-DTA curves of $LiCH_3CO_2 \cdot 2H_2O$ and $Mn(CH_3CO_2)_2 \cdot 4H_2O$ measured at a heating rate of 1℃/min under an oxygen flow.

acetate results in the second weight loss of 38.8% and two large exothermic DTA peaks around 250 ℃. This result agrees well with the calculated value, 39.0% for the release of $7.5H_2O$ and $10CO_2$, as well as the gain of $10.75O_2$. In this way, the reaction pathway can thus be given as follows:

$$LiCH_3CO_2 \cdot 2H_2O + 2Mn(CH_3CO_2)_2(4H_2O \rightarrow LiMn_2(CH_3CO_2)_5 + 10H_2O \quad \text{(Eq. 3)}$$

$$LiMn_2(CH_3CO_2)_5 + 10.75O_2\ R\ LiMn_2O_4 + 7.5H_2O + 10CO_2 \quad \text{(Eq. 4)}$$

The decomposition of both acetates around 250 ℃ releases massive heat. This exothermic heat is predicted to be utilized as the lattice energy required for the formation of $LiMn_2O_4$ phase. Like $LiNi_{0.7}Co_{0.3}O_2$, during the heating around 250 ℃, the decomposition of the acetates occurs, and 10 moles of CO_2 gas are simultaneously emitted.

TG-DTA curves of a mixture of $LiCH_3CO_2(2H_2O$ and $Co(CH_3CO_2)_2(4H_2O$ in Figure 3 ascertain that the first weight-loss (experimental value of 30.8%) between room temperature and 80 ℃ together with

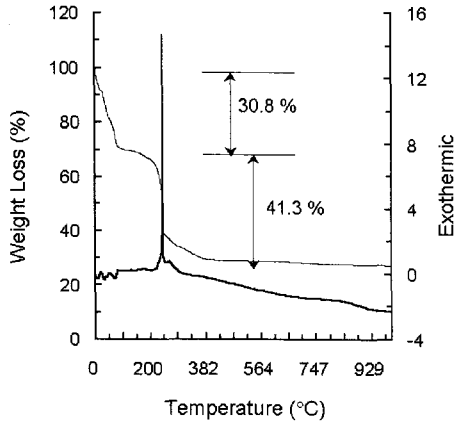

Figure 3. TG-DTA curves of a mixture of $LiCH_3CO_2 \cdot 2H_2O$ and $Co(CH_3CO_2)_2 \cdot 4H_2O$ measured at a heating rate of 1℃ min^{-1}.

small endothermic DTA peaks up to 80 ℃ correspond to the removal of hydrated $6H_2O$ (theoretical value of 30.8%). Beyond 80 ℃ up to 350 ℃, decomposition of lithium acetate and cobalt acetate results in the second weight loss of 41.3% and a large exothermic DTA peak at 260 ℃. This result is exactly in accordance with the theoretical value, 41.3% for the release of $4.5H_2O$ and $6CO_2$, as well as the gain of $6.25O_2$. The decomposition of both acetates at 260 ℃ releases massive heat. This exothermic heat is predicted to be utilized as the lattice energy required for the formation of $LiCoO_2$. The reaction pathway can thus be given as follows:

$$LiCH_3CO_2 \cdot 2H_2O + Co(CH_3CO_2)_2(4H_2O \rightarrow LiCo(CH_3CO_2)_3 + 6H_2O \quad \text{(Eq. 5)},$$

$$LiCo(CH_3CO_2)_3 + 6.25O_2 \rightarrow LiCoO_2 + 4.5H_2O + 6CO_2 \quad \text{(Eq. 6)}.$$

While the temperature of 350 ℃ is the end-point for all of thermal weight loss, endothermic and exothermic, the practical temperature of the second weight loss and the huge exothermic heat is 260 ℃. During the heating around 260 ℃, the decomposition of both acetates occurs, and 6 moles of CO_2 gas are simultaneously emitted. Here, providing externally CO_2 gas during the self-emission of CO_2 gas promotes crystal nucleation and dispersion of crystal nuclei, but, at the same time, inhibits crystal growth.

The XRD patterns of nano-sized $LiNi_{0.7}Co_{0.3}O_2$, $LiCoO_2$, and $LiMn_2O_4$ are shown in Figure 4 and Figure 5. All XRD peaks of the prepared phases are characteristic for the reference phases.

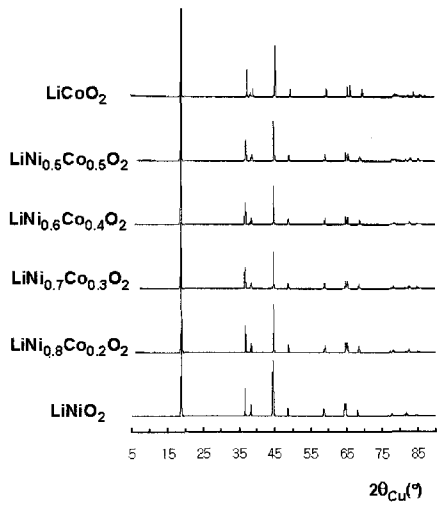

Figure 4. X-ray diffraction patterns for nano-sized $LiCoO_2$, $LiNi_{0.5}Co_{0.5}O_2$, $LiNi_{0.6}Co_{0.4}O_2$, $LiNi_{0.7}Co_{0.3}O_2$, $LiNi_{0.8}Co_{0.2}O_2$, and $LiNiO_2$.

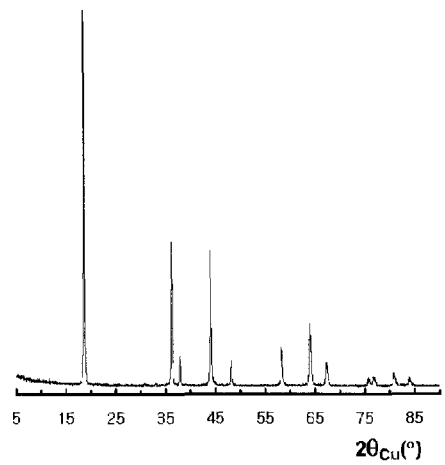

Figure 5. X-ray diffraction pattern for nano-sized $LiMn_2O_4$.

Respectively, Figures 6, 7, 8 show the SEM images of the morphologies in $LiNi_{0.7}Co_{0.3}O_2$, $LiMn_2O_4$, and $LiCoO_2$ prepared without external

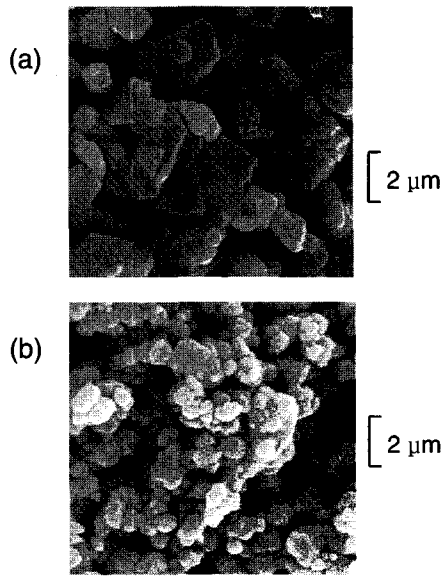

Figure 6. SEM images of (a) $LiNi_{0.7}Co_{0.3}O_2$ prepared without CO_2 stream, and (b) $LiNi_{0.7}Co_{0.3}O_2$ prepared in CO_2 pressure of 0.01 kgf/cm$_2$.

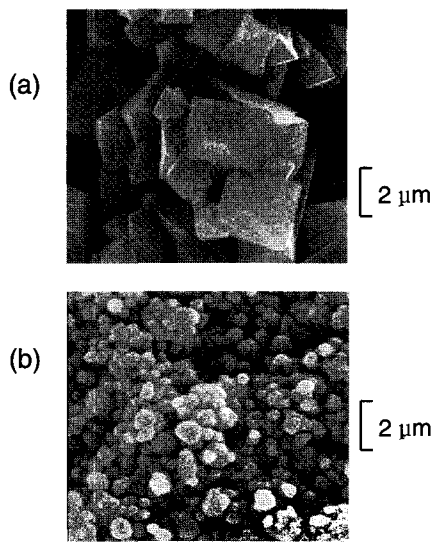

Figure 7. SEM images of (a) $LiMn_2O_4$ prepared without CO_2 stream, and (b) $LiMn_2O_4$ prepared in CO_2 pressure of 0.01 kgf/cm^2.

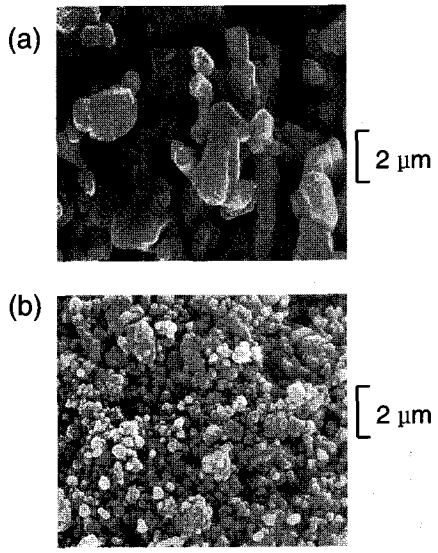

Figure 8. SEM images of (a) $LiCoO_2$ prepared without CO_2 stream, and (b) $LiCoO_2$ prepared in CO_2 pressure of 0.01 kgf/cm^2.

CO_2 stream, together with the SEM images of the morphologies in $LiNi_{0.7}Co_{0.3}O_2$, $LiMn_2O_4$, and $LiCoO_2$ prepared in the external CO_2 pressure of 0.01 kgf/cm^2. These images directly demonstrate the effect of the injection of external CO_2 gas on the particle size of $LiNi_{0.7}Co_{0.3}O_2$, $LiMn_2O_4$, and $LiCoO_2$. It is easily found that those particle sizes are significantly different. While the $LiNi_{0.7}Co_{0.3}O_2$, $LiMn_2O_4$, and $LiCoO_2$ prepared without external CO_2 stream consist of micro-sized particles, the $LiNi_{0.7}Co_{0.3}O_2$, $LiMn_2O_4$, and $LiCoO_2$ prepared with external CO_2 stream consist of nano-sized and aggregated grains. In fact, the aggregation of the nano-sized $LiNi_{0.7}Co_{0.3}O_2$, $LiMn_2O_4$, and $LiCoO_2$ is not in itself, but ascribed to a gold-coating on the nano-sized $LiNi_{0.7}Co_{0.3}O_2$, $LiMn_2O_4$, and $LiCoO_2$ before the SEM observation to prevent a flying of nano-sized $LiNi_{0.7}Co_{0.3}O_2$, $LiMn_2O_4$, and $LiCoO_2$.

As shown in Figures 9 and 10, the $LiNi_{0.7}Co_{0.3}O_2$ prepared in CO_2 pressure of 0.01 kgf/cm^2 exhibits the discharge capacities of 170.8 mAh/g at 0.1C and

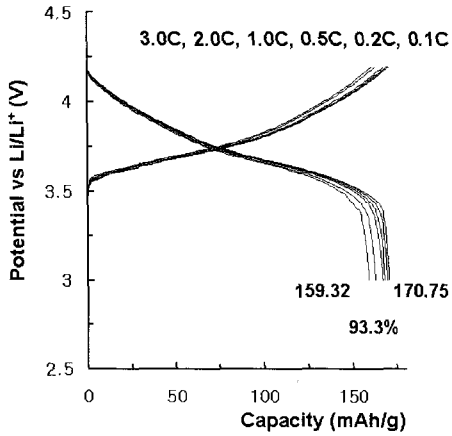

Figure 9. Voltage vs. capacity profiles of nano-sized $LiNi_{0.7}Co_{0.3}O_2$ at the 0.1C, 0.2C, 0.5C, 1.0C, 2.0C, and 3.0C.

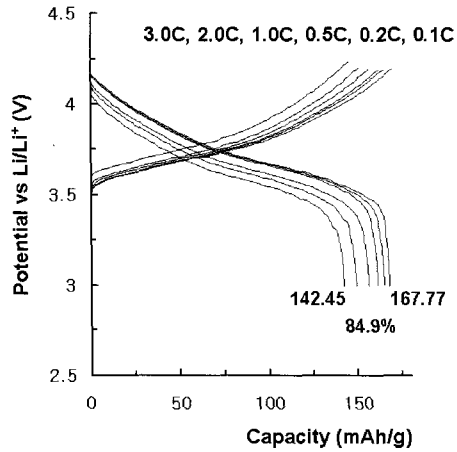

Figure 10. Voltage vs. capacity profiles of micro-sized $LiNi_{0.7}Co_{0.3}O_2$ at the 0.1C, 0.2C, 0.5C, 1.0C, 2.0C, and 3.0C.

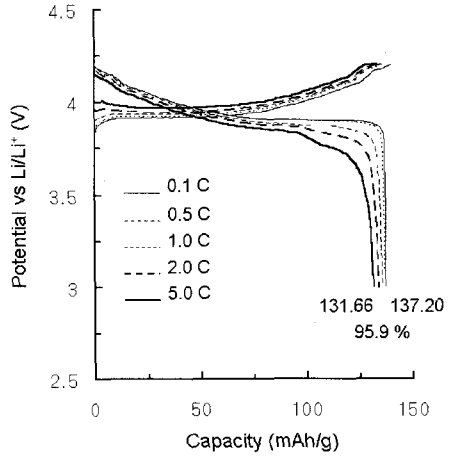

Figure 11. Voltage vs. capacity profiles of nano-sized $LiCoO_2$ at the 0.1C, 0.5C, 1.0C, 2.0C, and 5.0C.

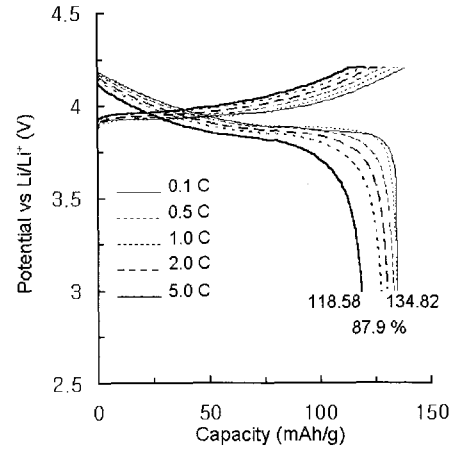

Figure 12. Voltage vs. capacity profiles of micro-sized $LiCoO_2$ at the 0.1C, 0.5C, 1.0C, 2.0C, and 5.0C.

159.3 mAh/g at 3.0C. However, the $LiNi_{0.7}Co_{0.3}O_2$ prepared without external CO_2 stream exhibits the discharge capacities of 167.8 mAh/g at 0.1C and 142.5 mAh/g at 3.0C. Needless to say, the difference in the high rate discharge capacity retentions of the two $LiNi_{0.7}Co_{0.3}O_2$ at 3.0C vs. 0.1C; 93.3 and 84.9 %, results from the effect of concentration polarization with those different particle sizes. On a $LiCoO_2$ system, the nano and micro-sized $LiCoO_2$ phases tend to exhibit very similar battery performances over and over. In Figures 11 and 12, the $LiCoO_2$ prepared in CO_2 pressure of 0.03 kgf/cm^2 exhibits the discharge capacities of 137.2 mAh/g at 0.1C and 131.7 mAh/g at 5.0C. However, the $LiCoO_2$ prepared without external CO_2 stream exhibits the discharge capacities of 134.8 mAh/g at 0.1C and 118.6 mAh/g at 5.0C. It means that the nano-sized $LiCoO_2$ has the high rate discharge

capacity retention at 5.0C vs. 0.1C of 95.9. And, that of micro-sized $LiCoO_2$ is 87.9 %. Although nano-sized cathode materials are economically and easily prepared by just direct thermal reaction without any artificial mixing procedures of reactants and ultra-miniaturization of products, those battery performances are on the whole excellent.

4. Conclusion

Nano-sized cathode materials for lithium ion polymer batteries are manufactured using united eutectic self-mixing method without any artificial mixing procedures of reactants and ultra-miniaturization of products. During the thermal reaction, just providing externally CO_2 gas promotes crystal nucleation and dispersion of crystal nuclei, but, at the same time, inhibits crystal growth, which results in material preparation and simultaneous ultra-miniaturization in a nano-size. The prepared nano-sized cathode materials exhibit excellent battery performances such as a discharge capacity retention at high rate.

Acknowledgements

This work was funded by Korea Research Foundation Grant (KRF-2001-005-E00033).

References

1. H. K. Kang, B. Y. Jung, M. G. Kim, Y. Lee, D. M. Kim, K. S. Ryu, K. S. Han, *Solid State Ionics,* **169**, 151 (2004).
2. B. Y. Jung, H. K. Kang, I. Jeong, K. S. Han, J. B. Choo, K. S. Ryu, *Electrochimica Acta*, **50**, 473 (2004).
3. S. W. Lee, B. Y. Jung, K. S. Han, Y. Lee, D. M. Kim, M. G. Kim, K. S. Ryu, E. Y. Kang, J. H. Jeong, *Electrochimica Acta*, **50**, 479 (2004).
4. Y. Lee, A. J. Woo, K. S. Ryu, Y. J. Park, B. Y. Jung, J. H. Lee, K. S. Han, *Solid State Ionics*, **175**, 311 (2004).
5. K. S. Ryu, Y. Lee, K. S. Han, M. G. Kim, *Materials Chemistry and Physics*, **84**, 380 (2004).
6. Y. J. Heo, Y. K. Kang, K. S. Han, C. J. Lee, *Electrochimica Acta*, **50**, 345 (2004).
7. S. S. Choi, Y. S. Lee, C. W. Joo, S. G. Lee, J. K. Park, K. S. Han, *Electrochimica Acta*, 50, 339 (2004).